Quantification of Atomic Force Microscopy tip and sample thermal contact

This manuscript was accepted by Rev. Sci.Instrum. Click here to see the version of record.

Zarina Umatova*[a], Y. Zhang [b], Ravishkrishnan Rajkumar [b], Phillip S. Dobson[c], J.M.R. Weaver[c]

[a] Nazarbayev university, 153 Kabanbay batyr Avenue, Astana, Kazakhstan, 010000
[b] Kelvin Nanotechnology, Oakfiled Avenue, Glasgow, UK, G12 8LT
[c] University of Glasgow, Oakfiled Avenue, Glasgow, UK, G12 8LT

A thermal conduction measurement device was fabricated, consisting of a Silicon dioxide membrane with integrated thermal sensors (Pt resistance heater / thermometer and Pt-Au thermocouples) using MEMS technology. Heat transfer between the heated device and a number of unused Atomic Force Microscope and Scanning Thermal Microscope probes was measured and changes in thermal conduction related to changes in the tip shape resulting from initial contact. The sensors were fabricated by electron beam lithography and lift-off followed by local subtractive processing of a Pt-Au multilayer to form Pt heater – resistance thermometer elements and Pt – Au thermocouples. Thermal isolation from the silicon substrate was provided by dry release of the supporting 50nm thick SiO2 membrane using an isotropic SF6 ICP plasma etch. The high thermal isolation of the sample combined with the sensitivity of the temperature sensors used allowed the detection of thermal conduction between tip and sample with high precision. The measured temperature range of Pt resistor was 293-643K. The measured thermal resistance of the membrane was 3×10^5 K/W in air and 1.44×10^6 K/W in vacuum. The tip contact resistance was measured with a noise level of $0.3g_0 T$ at room temperature, where g_0 is the thermal resistance quantum.

1. Introduction

The Scanning Thermal Microscope (SThM) is one of the most flexible tools available for measuring thermal transport at the nanoscale. However, heat transfer between the probe and sample has a complicated nature as it depends on different parameters such as the nature of the surrounding gas (pressure, temperature, degree of humidity), and that of the mechanical contact between probe tip and sample (surface roughness and topography, mechanical properties of the tip surface and sample surface and the force applied). So understanding the heat flow between tip and sample requires careful study of all of these parameters. Thus quantification of tip and sample thermal contact is a key problem in the interpretation of SThM measurements.

Measuring heat conductance between SThM/AFM tip and sample is main objective of this work. Measuring this small conductance requires the sensible

numbers for scaling and expressing these values. By expressing the heat conductance in terms of thermal conductance the obtained values will be expected to be a small multiple of conductance quantum g_0. The phonon transport in a one-dimensional channel at low temperature was studied by Schwab et.al. [1] Where the thermal conductance approaches a minimum value, which is called the universal quantum of thermal conductance g_0. This represents the value of energy transported per phonon mode in ideal coupling between a ballistic thermal conductor and a reservoir, so that the modal transmission coefficients are equal to unity. This assumption leads to a fundamental relation for the quantum of thermal conductance [1] which can be represented by

$$g_0 = \pi^2 k_b^2 T/(3h), \qquad \textbf{(1)}$$

Where k_b is Boltzmann's constant, T is the temperature in kelvin and h is Planck's constant. Substitution gives a value of

$g_0 = (9.45\times10^{-13} W/K^2)T$

$= 2.839\times10^{-10}$ W/K at room temperature. The room temperature value of g_0 will be assumed throughout this work.

Another reason for using this scaling is to investigate whether thermal conduction through the contact is quantized. In some experiments, these contacts have been found to be quantized [2], and in some there is no evidence of strong quantization.[3] In the present work, although the variation in conduction was step-like, the size of the steps was not found to be simply related to g_0.

In order to measure thermal characteristics using SThM is important to understand the temperature distribution within cantilever and tip

* Zarina.umatova@nu.edu.kz

This manuscript was accepted by Rev. Sci.Instrum. Click here to see the version of record.

when brought into contact with sample surface.

The heat from a heated SThM tip goes through the cantilever, surrounding gas, through solid-solid mechanical contact and the water meniscus. [4], [5], [6].

When a cold (unheated) probe is brought into contact with heated sample this is called "passive mode" SThM (Figure 1) and is commonly associated with the use of SThM in thermometry applications.

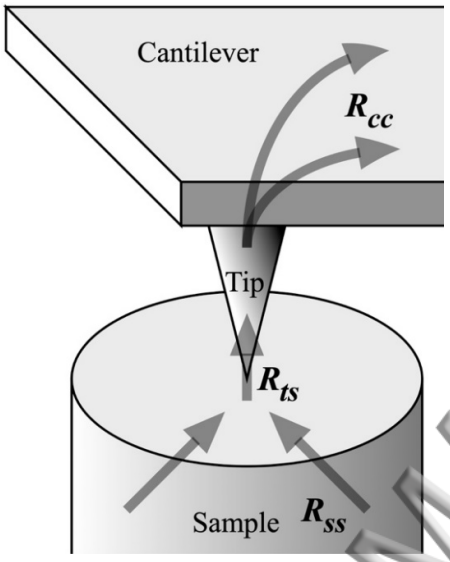

Figure 1 Heat distribution in Passive mode in vacuum: R_{ss} is the thermal spreading resistance in the sample, R_{ts} is the thermal resistance at the tip-sample junction and R_{cc} is the thermal resistance due to conduction along the cantilever

In passive mode, an unheated tip scans along the heated active sample. A very small current (for example, about *I = 1-2 mA* for Wollaston wire probe[7] and *0.1 mA* for a KNT probe[8], [9]) is passed through the probe, in order to minimize Joule heating whilst still allowing measurement of the electrical resistance and hence temperature of the sensor. It should be noted that the temperature of the sensor is not the same as the temperature of the sample. Rather, the temperature of the sensor (which is situated near to the apex of the probe) will be intermediate between that of the sample and the microscope to which the cantilever is attached. The temperature of the sensor will be determined by the thermal resistances connecting it to these large thermal reservoirs.

Various self-heated samples have been fabricated in order to quantify heat transfer between probe and tip in passive SThM mode. [10], [8] Some of these self-heated samples have been designed and fabricated specifically for absolute temperature measurements on the micrometre scale. One which was fabricated for calibration of a nano-thermometer (SThM probe) with accuracy better than 1K on the scale of one micron was based on the use of the measurement of Johnson noise (P. S. Dobson et.al [9].)

Johnson noise is a primary standard of temperature. [11] The Johnson noise device was demonstrated as an accurate calibration device; however, it suffered from some thermal nonuniformity due to its asymmetric wiring onto the silicon substrate. An improved device having a more symmetric configuration, which offered maximum temperature uniformity at the device centre, was fabricated by Ge et.al. [8] The device was designed, fabricated and characterised using SThM to provide an accurate and spatially variable temperature distribution that could be used as a temperature reference. Thermal conductance between the SThM tip and active sample was determined as $\mathbf{1.2 \times 10^{-6}}$ W/K in air. In use this sample demonstrated a significant residual asymmetry in the temperature measured using SThM. This was determined to be due to direct thermal conduction between cantilever and sample through the air. As such conduction does not give a good localisation of measurement recent work on thermometry has focussed on operation in vacuum. One of the most accurate attempts at Temperature quantification by the self-heating of silicon nanowires in vacuum was performed by Menges et.al. [5] The thermal resistance of the tip-surface contact was measured at DC and then the local temperature was determined from the AC heat flow. The capability of scanning thermal microscope to determine the temperature distribution quantitatively on nanometre scale with a resolution on the order of 20-30 K at approximately 25 nm lateral resolution was shown. However, there are some limitations on the method demonstrated. . The sensitivity of the temperature

This manuscript was accepted by Rev. Sci.Instrum. Click here to see the version of record.

measurements is limited by the resistance measurements of the heater with when scanning in contact mode.[5] The thermal-spatial resolution of that experiment was also limited by the temperature gradient of the sample itself and also by the wear robustness of the SThM tip sliding on silicon oxide during the scan. [5].

Another issue, which needs to be considered in sample- probe tip contact, is surface roughness at the nanoscale because the effective value of the contact radius can change depending on that factor. As described by Gotsmann et. al. [2], heat transport across multiple nanoscale contacts between an SThM tip and sample was seen as a pressure dependence of thermal transport across a polished nanoscale contact. Finally, the effect of different materials on the interfacial resistance is an important factor to consider. In particular the effect of surface water films was expected to lead to significant variability in the conduction between surfaces having the same composition and roughness. It was therefore decided to make measurements of thermal conduction between tip and sample under vacuum during this work. [4].

The heat flow between the tip-sample or sample – tip in vacuum is simpler than that in air, since all of the heat is transported via the tip-sample contact. The power transferred can be written as

$$P_{t-s} = \frac{\Delta T}{R_{ss} + R_{ts} + R_{cc}} = g_{t-s}\Delta T \qquad (2)$$

Where the quantities R_{ss}, R_{ts} and R_{cc} are defined in Figure 1, ΔT is the temperature difference between sample and cantilever, $g_{t\text{-}s}$ is the total thermal conductance between sample and probe and $P_{t\text{-}s}$ is the power flowing between sample and probe. The significant variable in SThM measurements is R_{ts}.

Fabrication

A sample specifically designed to study low dimensional heat transport between SThM tip and sample surface was made using nanofabrication and MEMS technology.

The fabrication process comprises 3 stages: defining the individual chips and alignment structures, active device fabrication and thermal isolation of the membrane supporting the devices from a heat sink.

Two contact photolithography and three electron-beam lithography levels were patterned on the wafer to construct the device. The photolithography steps were used to define the individual dice and for alignment from front to back of the electron-opaque silicon substrate. Electron-beam lithography was used to define the contact structures and sensors having widths of approximately 200nm due to its resolution [12], and to open the holes in the SiO_2 membrane which required accurate size and alignment. The whole process for active device fabrication is presented in the diagram shown in Figure 2. The thermal isolation of the membrane was achieved using isotropic dry etch. A tilted SEM image of the final device is shown in **Figure 3**. It is clear from the image that membrane is fully released from the Silicon substrate.

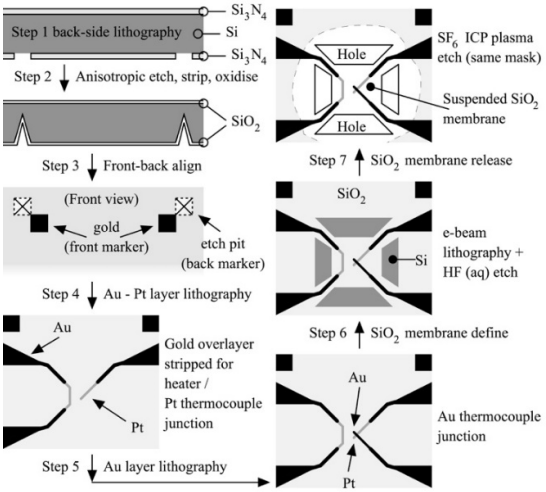

Figure 2 The fabrication process of active device.

1. Photolithography I (back side) for defining cleaved lines with Si_3N_4 dry etch. 2 Wet etch (anisotropic etch of Si) then stripping Si_3N_4 and dry thermal oxidation. 3.Photolithography and gold marker lift-off for aligning back side to front side of the wafer. 4.Pt Au bilayer patterned by e-beam lithography to define Pt heater-thermometer and half thermocouple: Gold etched away in active areas, remaining on leads and pads 5. Second lead of thermocouple defined (Au).6. Windows to define membrane edges and supports defined by e-beam lithography andaqueous HF etching. 7. Isotropic Si dry etch using same mask as 6 to undercut and release SiO_2 membrane.

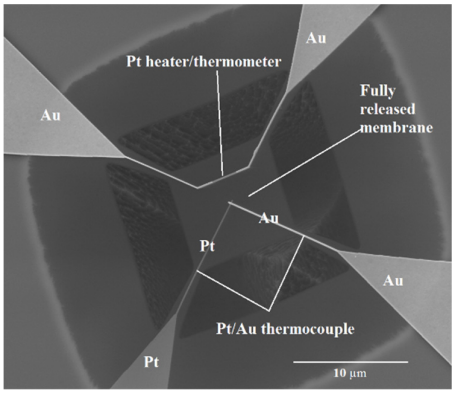

Figure 3 Final device showing platinum resistance and thermocouple sensors fabricated on the 50nm thick freestanding SiO_2 membrane. Undercut of the SiO_2 membrane by the isotropic SF_6 plasma etch is visible near the edge of the image

2. Measurements

The device was thermally calibrated in a series of experiments. Firstly the temperature coefficient of resistance of the sensor was determined using a resistance bridge whilst heating the sensor in a heated stirred bath of an inert liquid fluorocarbon, Perfluoro-1,3,-dimethylcyclohexane, trade name "Flutec PP3"[2]. This is a non contaminating, non toxic liquid at room temperature with an electrical resistivity in excess of 10^{11} Ω-m. Next the coefficient of self-heating in vacuum and sensitivity of the thermocouple were determined to be $1.49\pm0.04\times10^{6}$ K/W and 3.3 µV/K respectively by using the measured temperature coefficient of resistance and known power applied through the resistance bridge. The resistance of the probe was found to be stable in vacuum under self-heating for temperatures up to 643K. Above this temperature permanent changes in resistance were observed.

Thermal measurements in vacuum were obtained using a modified Nanonics MV400 AFM/SThM system. The device membrane was heated by passing a sinusoidal alternating current (AC) signal through to the Pt thermal sensor, which is used both as a resistance heater and a resistance thermometer detector (RTD). The 3ω signal (Voltage) change across the sensor which was part of a Wheatstone resistance bridge was measured as an unheated tip was brought into contact with it. [13]

AFM probes with different materials were used with the same device to investigate the dominant factors influencing the nature of the tip – sample heat transfer mechanism. The three type of probes used are the commercially available FESP probe[3] which is a sharp silicon AFM probe having a similar tip structure to the Anasys Thermal Lever probe[4][15][16], the KNT SThM probe[5], and a deprocessed Si_3N_4 KNT probe of the same type as the previous one but without any metallization. These were chosen to correspond to commonly used SThM probe types.

Approaching and retracting the tip to the sample was performed without using a laser force measurement system. An optical microscope was used to position the probe in the device plane ($x - y$) and to get the probe near to the surface before final approach using the z-piezo. (Figure 4) The tip-sample contact was detected by a step change in thermal conduction determined from the 3-ω signal. Thus thermal measurements could be made on probes from the very first contact of the previously unused probes to the device surface.

[2] F2 Chemicals Ltd. Lea Lane, Lea Town, Nr. Preston Lancs. PR40RZ (UK)
[3] Bruker AFM probe, Bruker AFM Probes, 3601 Calle Tecate, Suite C, Camarillo, CA 93012, FESP V-2
[4] Brucker USA (Atomic Force Microscopes)
112 Robin Hill Road
Santa Barbara, CA 93117
USA

[5] Kelvin Nanotechnology, 70 Oakfield Avenue, Glasgow, UK, G12 8LT, KNT-SThM-1an-5

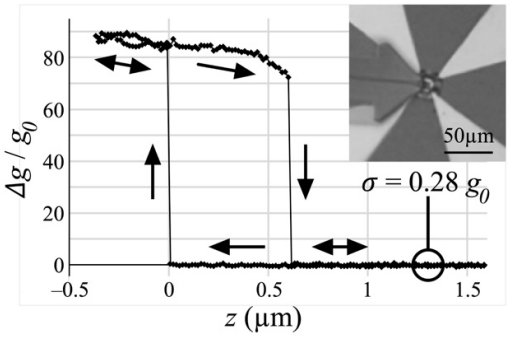

Figure 4 Thermal resistance change on first approach and retraction of a KNT probe to the device in vacuum. Note sudden change in conduction of 83.5g_0 and significant hysteresis due to pull-off force. Noise (standard deviation) out of contact is 0.28 g_0. Inset: optical image of probe before approach

A diagram of the geometry of tip and sample contact shown in Figure 5. The diagram defines the microscope coordinate system and shows how the sample and probe tip are mounted inside the chamber for contact.

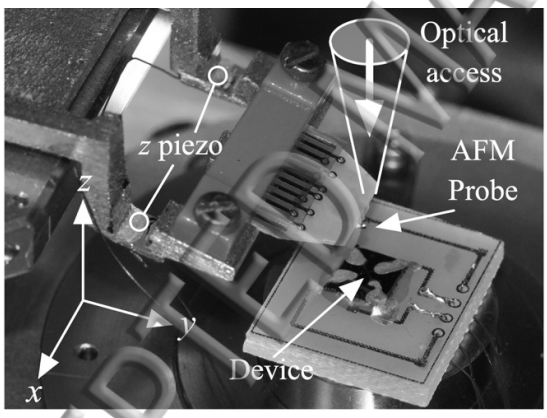

Figure 5 Geometry of tip and sample defining coordinate system used

Thermal sensors integrated on top of the thermally isolated membrane allow measurement of the thermal conductance between AFM probes and sample with very high precision thanks to the extreme sensitivity of the active device.

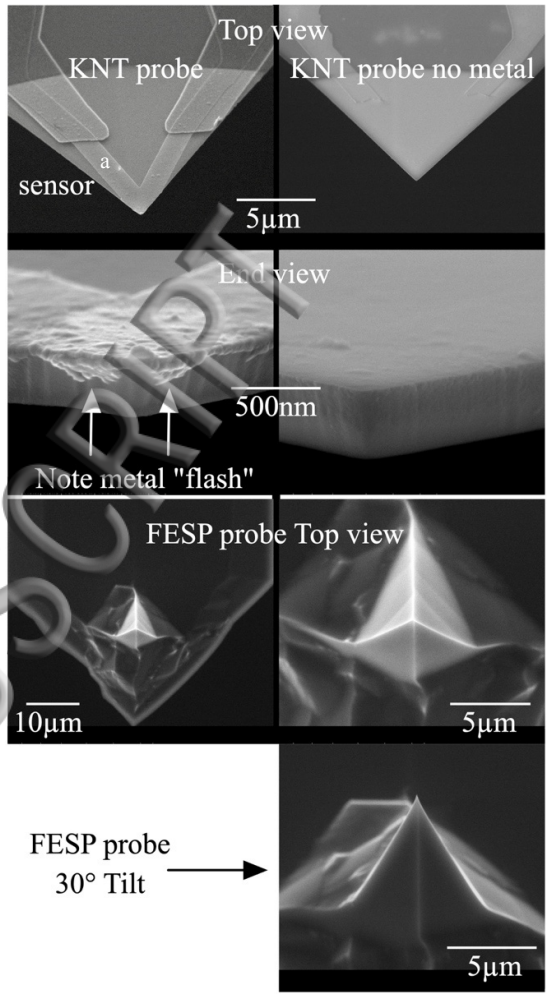

Figure 6 SEM image of all probes before contact

To gain understanding of the tip-sample contact the area and nature of the contact were important variables. The probes were therefore inspected using a scanning electron microscope before (Figure 6) and after measurements (Figure 8). SEM measurements were made using a "Helix" detector and reduced vacuum (0.3mbar H_2O) to avoid surface charging and contamination [14]

The first probe to be examined was the KNT SThM probe with a 400 nm thick silicon nitride transparent cantilever and a much blunter tip than the FESP. The resistance thermometer sensor consists of a coating of 5 nm NiCr and 40 nm palladium. Electrical contact to the sensor is made by thicker gold leads. These are the tips mostly

used for SThM so such measurements of tip-sample thermal conduction are of great practical importance. An important detail is that the palladium sensor is positioned at the end of the Si_3N_4 cantilever using a process of "self-alignment". During fabrication the sensor shape is defined in resist and the metallic sensor material evaporated onto the probe through the resist "stencil", which is then removed in a "lift-off" process. The extent of the metal at the tip is defined by the existing extent of the Si_3N_4 cantilever. This ensures that the sensor is present at the end of the tip, but results in unavoidable deposition of a thin metallic coating, or "flash", on the end of the probe as seen in Figure 6.

A second probe type was another KNT SThM probe in which the sensor material had been chemically etched from the cantilever. This sample was used as it had the same sharpness as the KNT probe, but, like the FESP probe, was composed of a single material.

A third type of probe is the FESP Si probe, which has a sharp silicon tip similar to that of doped silicon SThM probes, so it can be used as proxy to investigate the thermal character of the tip to sample contact of such probes. The distinguishing feature of this probe is that it is initially very sharp, beyond the resolution of the SEM used.

The device was biased and the unheated probes were brought into contact with it one after another under high vacuum conditions. The results are presented in Figure 7. The total range of motion after first contact for the three probes was approximately equal, being 380, 550 and 400nm respectively for the three probe types. Using the value of stiffness of the device which was calculated by finite element modelling to be 0.106 N/M and the specified values of stiffnedd for the AFM and SThM probes used (2.8 N/M for FESP and 0.25 N/M for the KNT probe and cantilever) this corresponds to peak forces of 28 nN, 41 nN and 41nN for the three probe types.

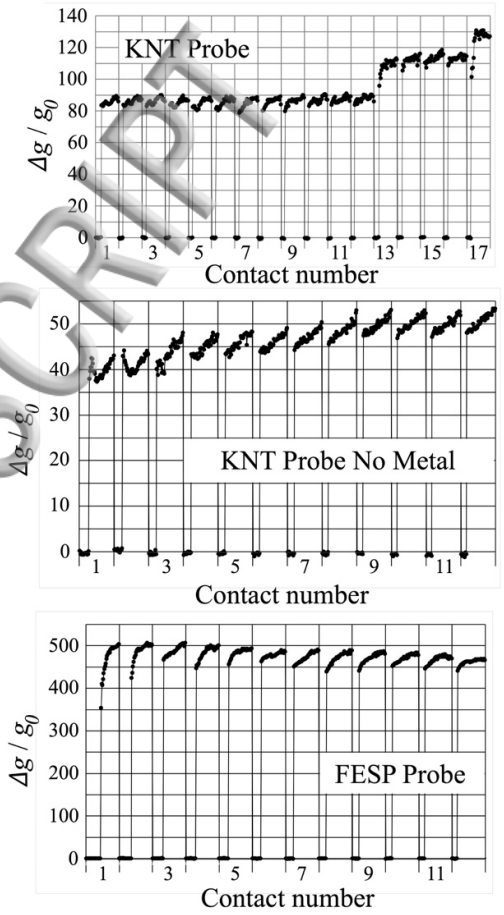

Figure 7 Thermal conduction in units of the room-temperature thermal conductance quantum for successive contacts of the three types of probe from initial contact of an unused probe (contact 1). Data plotted during approach only.

Examining Figure 7, in the case of the KNT SThM probe the thermal conductance abruptly rises to a value of some 83 times the thermal resistance quantum at room temperature, or 24 nW/K on first contact. As might be expected for such a blunt probe, the change in conductance is seen to be relatively slight with increasing force (about 5% increase from first contact to peak force), and the variation of initial thermal conduction in

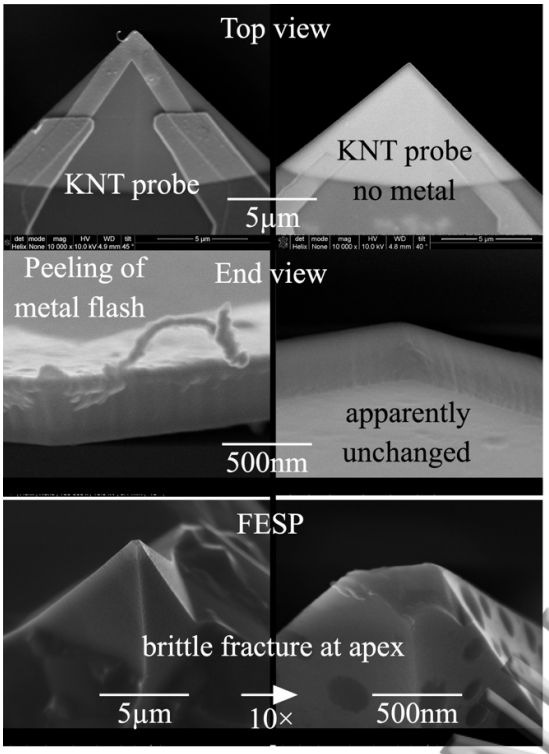

Figure 8 The same probes shown in Figure 6 after measurements have been completed. The gross change in the form of the metalization of the KNT probe may be seen by comparison with Figure 6. The unmetallized KNT probe is apparently unchanged. The FESP probe has been significantly blunted by a brittle fracture process.

subsequent contacts is small, ranging from 78.6-83.9 g_0 in the first 12 contacts. At the 13th contact the nature of the contact abruptly changes to a value of 105 g_0 with a strong distance dependence of about 0.23 g_0 / nm, rising to a peak stable conductance of some 113.4 g_0. After four cycles of contact, at contact 17 the nature of the contact again changes, with a peak conductance of about 129 g_0. Examination of the SEM images taken after the 17th approach (Figure 8) shows that the probe has suffered a significant mechanical change. A small length of the "flash" from the sensor metal deposition has detached from the tip of the probe and is assumed to be making a second thermal contact to the sample.

The KNT probe in which the metal was removed gave a much smaller thermal conductance on first contact of 38.0 g_0 despite being of similar sharpness to the KNT SThM probe. This might be reasonably explained by the lower thermal conductivity of Si_3N_4 compared to palladium. The Curve is observed initially to decrease slightly in thermal conductance with applied force for the first two contacts, but thereafter the curve tends to a relatively reproducible form, having an initial conductance of 48.1 g_0 and a slope of 8×10^{-3} g_0 / nm. Comparison of SEM images before and after scanning show no discernible change in probe morphology. The slight change in the form of the curve after a small number of contacts might therefore reasonably be ascribed to the displacement of initial contamination or the "polishing" of the surface of the tip at a scale which is not apparent to SEM investigation.

The final probe type to be investigated is the FESP probe. The probe had the highest overall thermal conduction of any of the three probes investigated, with an initial conductance of 354 g_0 on first contact, despite the smaller contact area. A partial explanation of this result may be attributed to the difference in thermal conductivity between LPCVD Si_3N_4 and pure silicon, which have been reported to be of order 8 W/m/K [19] and 150 W/m/K respectively at room temperature, although both numbers are subject to wide variation depending on the precise nature of the materials used. On first contact the probe demonstrates an exceedingly rapid increase in thermal conductance of 3.55 g_0 / nm, which would be indicative of a very sharp tip. On the next contact the conductance starts at a higher level, although the latter part of the curve has a similar form, but for all subsequent contacts the thermal conductance is high on contacting, with a slow variation with pressure and very consistent values of conductance, indicative of a blunt probe. The observed behaviour is entirely consistent

with the "before" and "after" contact SEM images presented in Figures 6 and 8. The tip, which initially was too sharp to resolve in the SEM has become significantly blunter, having a flat apex of approximately 500nm width.

Summary

The nature of the tip-sample contact is a matter of extreme importance in scanning probe applications. In the case of SThM the thermal conductance of the tip-sample contact is a major cause of uncertainty in the determination of temperature or materials thermal properties. The instrument described provides an insight into such contacts with direct relevance to the practice of Scanning Thermal Microscopy.

Firstly, and perhaps most importantly, the observation of large changes in the nature of the contact when a pristine probe is introduced to a sample, even without any lateral scanning, might suggest that the use of very sharp probes in SThM (which is by nature a contact microscopy technique) is of limited utility. Indeed, the fact that the conductance values for the sharp FESP probe became stable and relatively insensitive to pressure after damage during the first contact would suggest the process of tip modification appears to be self-limiting. A deliberate blunting of probes, either during fabrication or by aggressive scanning might therefore be advantageous when performing quantitative measurements. Thus it is proposed that the design and fabrication of a silicon probe with a smooth blunt tip like a sphere with a radius of a few hundred nanometres would be a possible (if partial) solution to the variability of tip-sample contact using silicon probes.

In the case of functionalised Si_3N_4 cantilevers, the mechanical and thermal stability of the relatively blunt probe with no sensor seems to argue in favour of the use of a smooth and homogeneous probe for quantitative measurement. Of course, the incorporation of a sensor with such a cantilever is essential for the performance of thermal measurements, however, and this introduces a number of problems. Firstly, the use of self-alignment leads to the deposition of small regions of poorly-adhered metal on the vertically etched surface of the probe tip, and means that the top (sensor) side of the apex is composed of a different material to that of the other. In practice some redress may be obtained by "rough" scanning of a new probe to arrive at a stable shape and composition. From the standpoint of probe fabrication, the sensor might advantageously be modified to use explicit alignment methods, positioning the sensor a small distance from the tip and giving a pure Si_3N_4 surface with which to contact the sample. Alternatively, metal might be thickly deposited over the whole end of the sensor to give better thermal conductance to the sample than that obtained using Si_3N_4, or an isotropic encapsulating layer might be deposited onto the probe using a technique such as ALD.

The question of the state of the contact between tip and sample is of wider importance than SThM. The instrument itself has great potential utility as an addition to scanning probe microscopy of all types in a vacuum environment. The device itself provides a route to the performance of nanoscale thermal measurements without the need to use a dedicated SThM system. With a demonstrated noise level of 0.3 g_0 at room temperature, the potential for accurate calibration and excellent stability over time with a largely featureless extent of 10µm square the device could be used as a substrate for the deposition and attachment of elements using other scanned probe techniques. Since the system is sensitive to changes in morphology and contact on the nm scale it

lends itself to tribological studies and studies involving contact to nanometre scale clusters and objects. The ability to make a stable and quantitative measure of the state of contact between a probe and sample using such a non-invasive measure as thermal conductance simultaneously with conventional nanoscale measures (such as adhesion and stiffness) would provide extra information with a potentially small impact on the experiment being performed.

Acknowledgements

The authors would like to acknowledge the support of the Bolashak International Scholarship of the President of the Republic of Kazakhstan, the staff of the James Watt Nanofabrication Centre, EPSRC grant EP/J010774/1 and EU project "QUANTIHEAT" (Grant Agreement No. 604668) for its financial support.

Bibliography

[1] G. Electrostatic, K. Schwab, E. A. Henriksen, J. M. Worlock, and M. L. Roukes, "Measurement of the quantum of thermal conductance," *Nat. Mater.*, vol. 1275, no. 1997, pp. 1997–2000, 2000.

[2] B. Gotsmann and M. a. Lantz, "Quantized thermal transport across contacts of rough surfaces," *Nat. Mater.*, vol. 12, no. 1, pp. 59–65, 2012.

[3] Aritra Banerjee, Sudipta Pal1, E Rozenbergand B K Chaudhuri1, "Adiabatic and non-adiabatic small-polaron hopping conduction in La1−xPbxMnO3+δ (0.0 ≤ x ≤ 0.5)-type oxides above the metal–semiconductor transition," *J. Phys. Condens. Matter*, vol. 13, Feb. 2001.

[4] A. Assy, S. Lefèvre, P.-O. Chapuis, and S. Gomès, "Analysis of heat transfer in the water meniscus at the tip-sample contact in scanning thermal microscopy," *J. Phys. D. Appl. Phys.*, vol. 47, no. 44, p. 442001, 2014.

[5] F. Menges, H. Riel, A. Stemmer, and B. Gotsmann, "Quantitative thermometry of nanoscale hot spots," *Nano Lett.*, vol. 12, no. 2, pp. 596–601, 2012.

[6] S. G. Assy, Ali, "Heat transfer at nanoscale contacts investigated with scanning thermal microscopy," *J. Appl. Phys.*, vol. 107, no. 43105, 2015.

[7] B. Cretin, "Scanning Thermal Microscopy," *Europhys. News*, vol. 28, no. 1, pp. 29–29, 1997.

[8] Y. Ge, Y. Zhang, J. A. Booth, J. M. R. Weaver, and P. S. Dobson, "Quantification of probe–sample interactions of a scanning thermal microscope using a nanofabricated calibration sample having programmable size," *Nanotechnology*, vol. 27, no. 32, p. 325503, 2016.

[9] P. S. Dobson, G. Mills, and J. M. R. Weaver, "Microfabricated temperature standard based on Johnson noise measurement for the calibration of micro- and nano-thermometers," *Rev. Sci. Instrum.*, vol. 76, no. 5, 2005.

[10] P. S. Dobson, J. M. R. Weaver, and G. Mills, "New methods for calibrated Scanning Thermal Microscopy (SThM)," *Proc. IEEE Sensors*, pp. 708–711, 2007.

[11] M. Pumarol, M. C. Rosamond, P. D. Tovee, M. C. Petty, D. A. Zeze, V. I. Falko, and O. V Kolosov, "Direct nanoscale imaging of ballistic and diffusive thermal transport in graphene nanostructures Direct nanoscale imaging of ballistic and diffusive thermal transport in graphene nanostructures," *Metrologia*, vol. 52, 2015.

[12] B. S. Rao and U. Hashim, "Pattern transfer of 1µm sized microgap and microbridge electrode for application in biomedical nano-diagnostics," *Adv. Mater. Res.*, vol. 925, pp. 533–537, 2014.

[13] David G. Cahill, "Thermal conductivity measurement from 30 to 750K: the 3ω method" *Rev. Sci. Instrum.* **61**(2) pp. 802-808 (1990)

[14] B. L. Thiel, M. Toth, R. P. M. Schroemges, J. J. Scholtz, G. Van Veen, and W. R. Knowles, "Two-stage gas amplifier for ultrahigh resolution low vacuum scanning electron microscopy," *Rev. Sci. Instrum.*, vol. 77, no. 33705, pp. 1–7, 2006.

[15] W. P. King, B. Bhatia, J. R. Felts, H. J. Kim, B. Kwon, B. Lee, S. Somnath, and M. Rosenberger, "Heated Atomic Force Microscope Cantilevers and Their Applications," *Annu. Rev. Heat Transf.*, vol. 16, no. 1, pp. 287–326, 2013.

[16] J. Lee, T. Beechem, T. Wright, B. Nelson, S. Graham, and W. King, "Electrical, Thermal, and Mechanical Characterization of Silicon

Microcantilever Heaters," *J. Microelectromechanical Syst.*, vol. 15, no. 6, pp. 1644–1655, 2006.

[17] S. Poon ; J. Spièce ; A. Robson ; O.V. Kolosov ; S. Thompson, "Probing thermal transport and layering in disk media using scanning thermal microscopy," *IEEE*, 2017.

[18] P. D. Tovee, M. E. Pumarol, M. C. Rosamond, R. Jones, M. C. Petty, D. a. Zeze, and O. V. Kolosov, "Ultra High Thermal Resolution Scanning Probe Microscopy via Carbon Nanotube Tipped Thermal Probes," *Mesoscale Nanoscale Phys.*, pp. 1–21, 2013.

[19] X. Zhang and C. P. Grigoropoulos " Therrnai conductivity and cliff usivity of free-standing silicon nitride thin films" *Rev. Sci. Instrum.* **66**(2) (1995) pp. 1115-1120

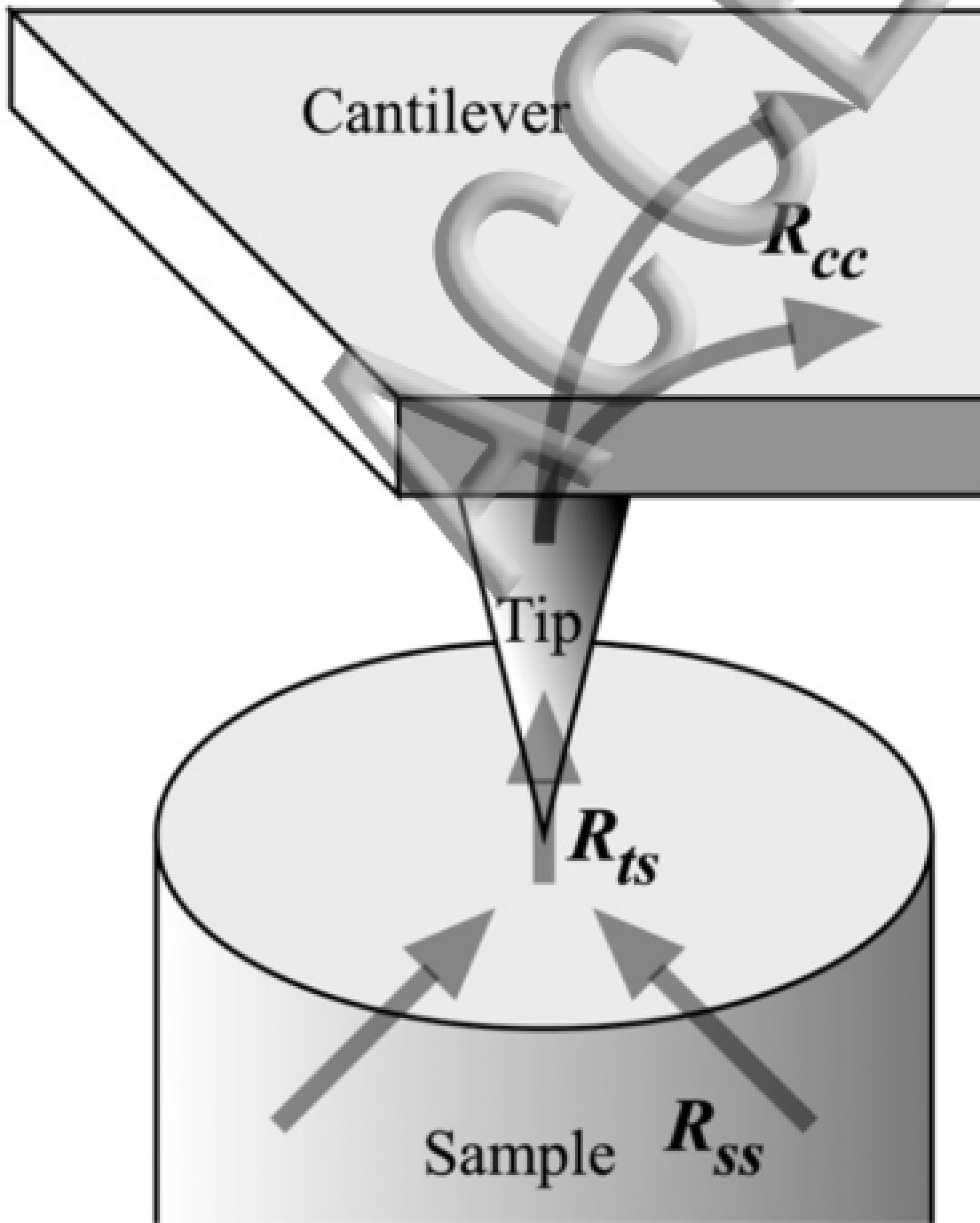
Cantilever
R_{cc}
Tip
R_{ts}
Sample
R_{ss}

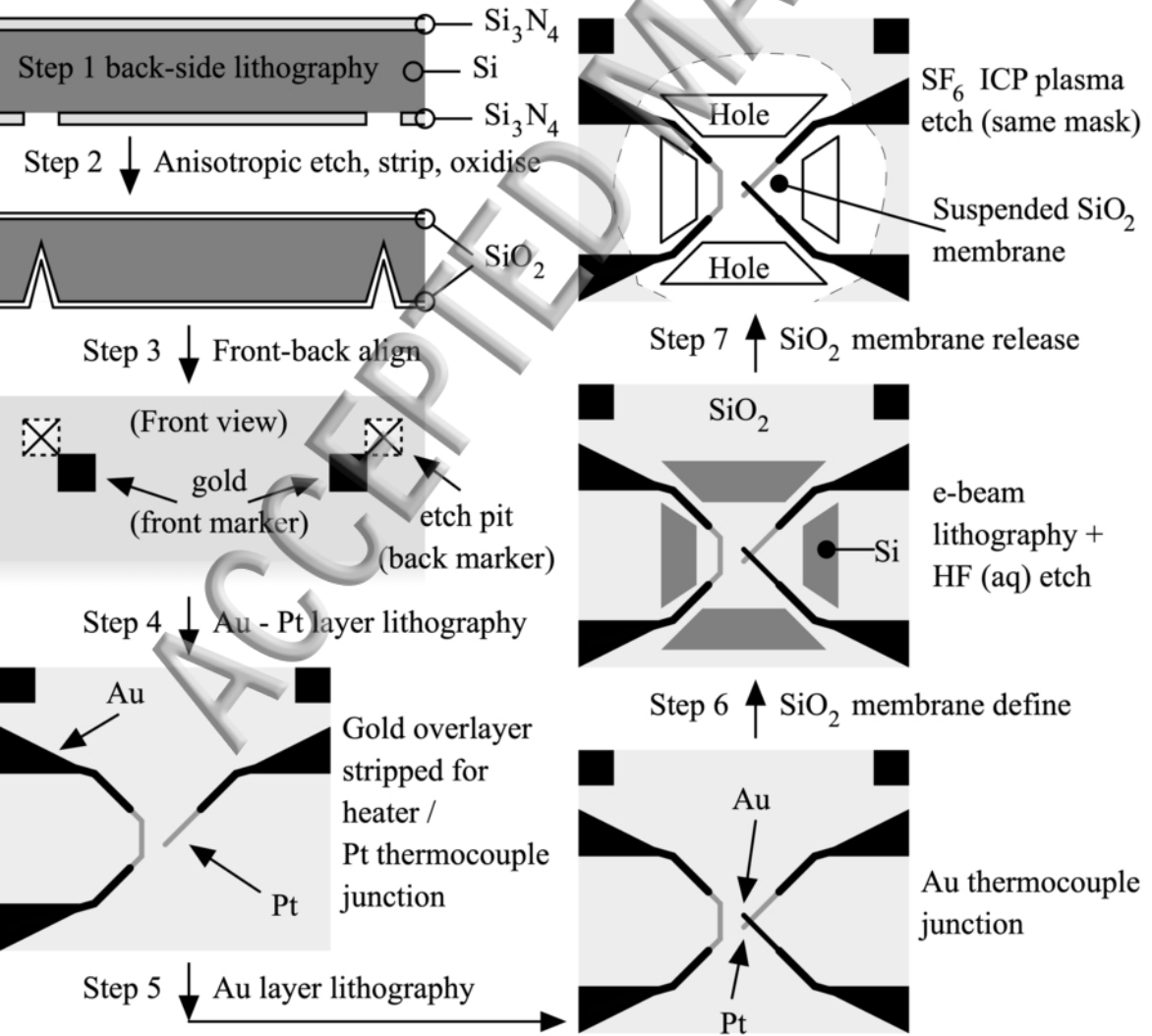

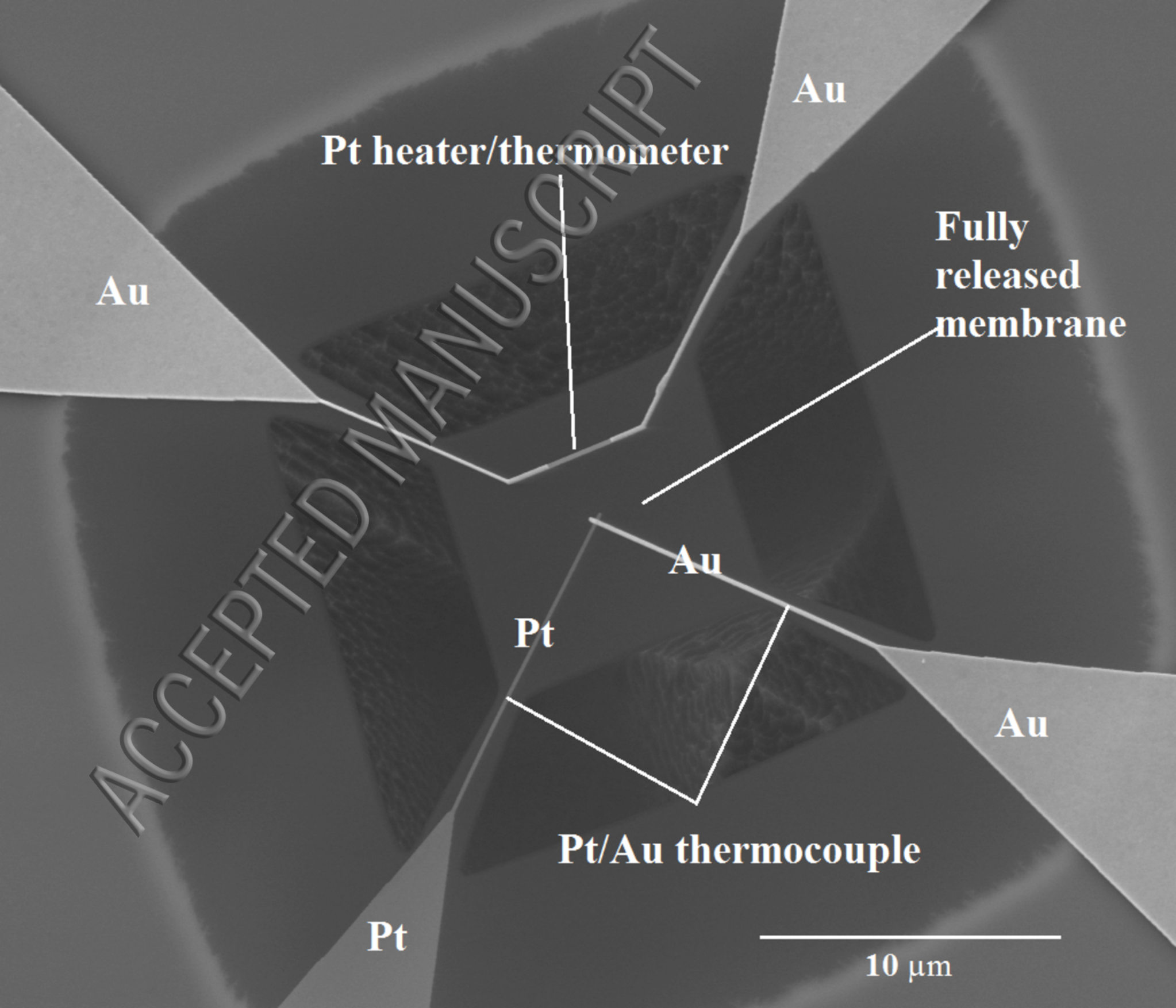

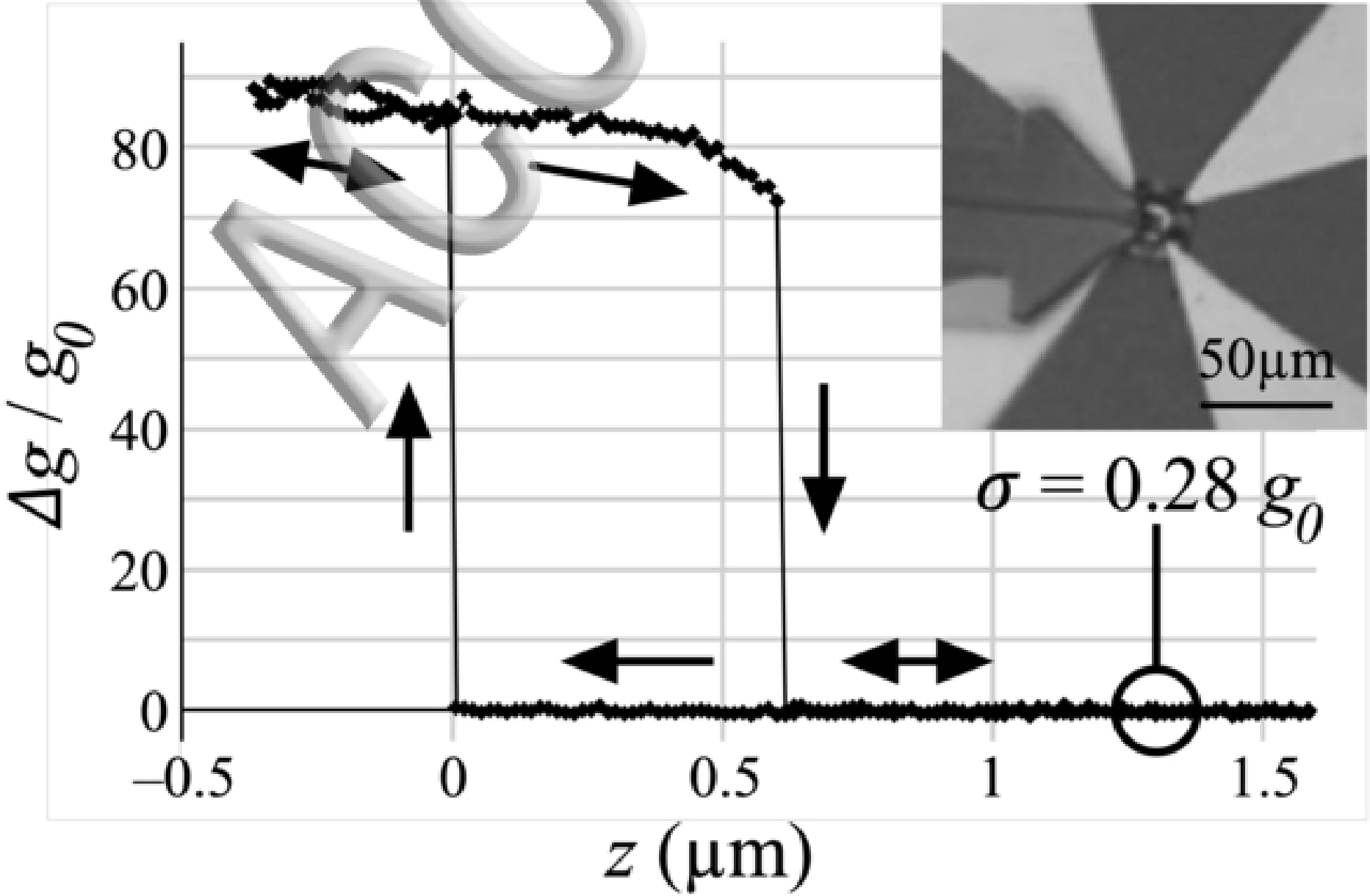
80
60
40
20
0
$\Delta g / g_0$
–0.5
0
0.5
1
1.5
z (μm)
$\sigma = 0.28\ g_0$
50μm

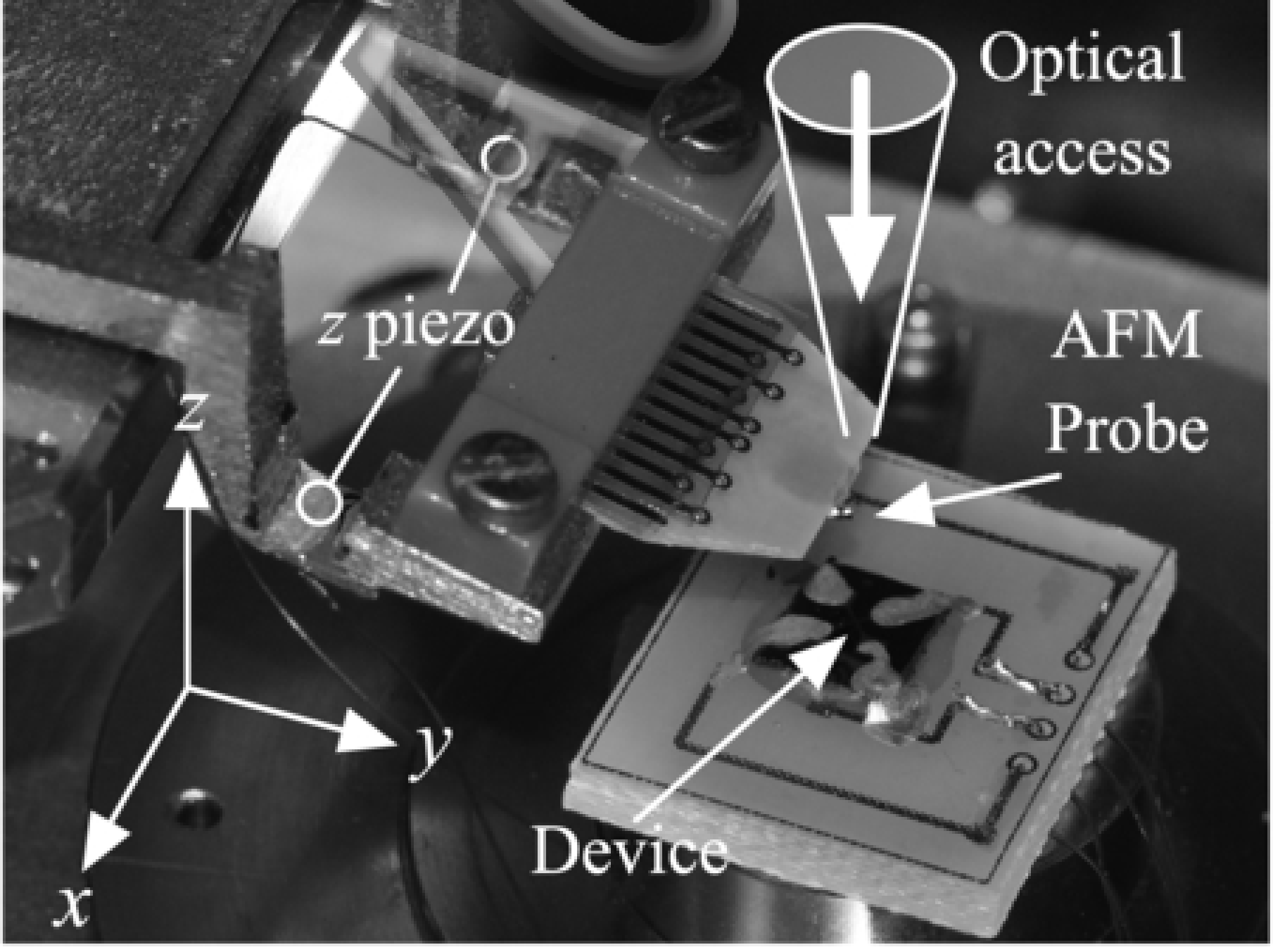
Optical
access
z piezo
AFM
Probe
z
y
x
Device

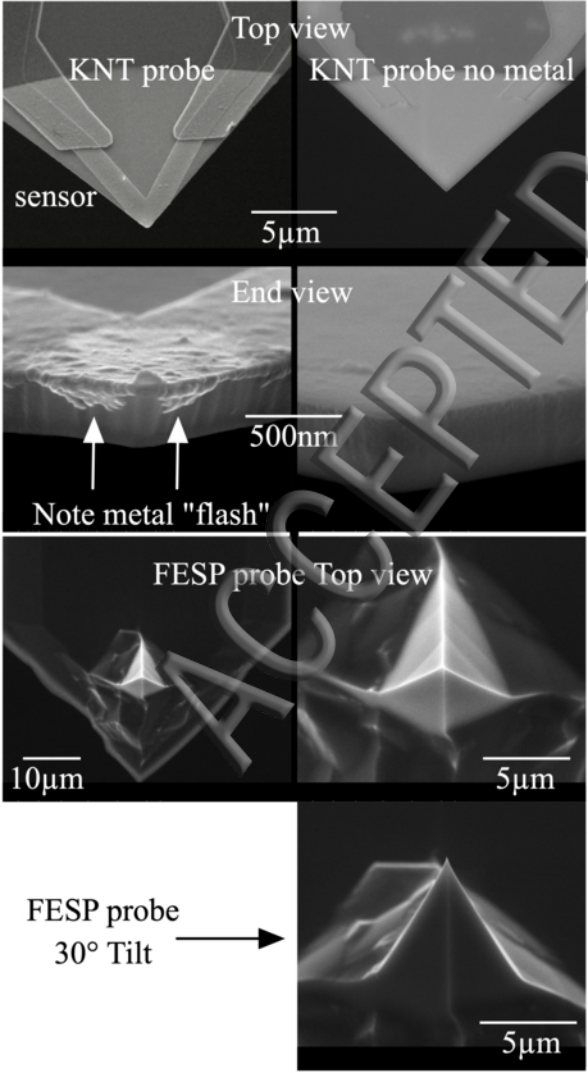
Top view
KNT probe
KNT probe no metal
sensor
5µm
End view
500nm
Note metal "flash"
FESP probe Top view
10µm
5µm
FESP probe
30° Tilt
5µm

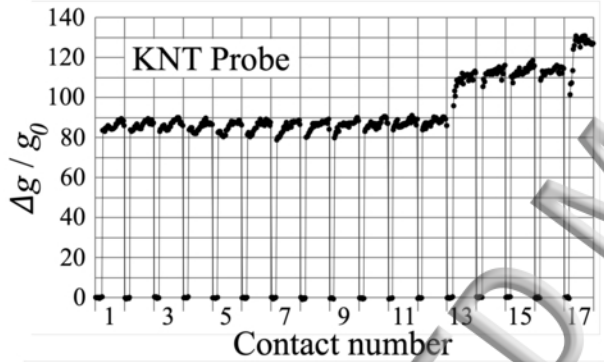
KNT Probe
Δg / g0
Contact number

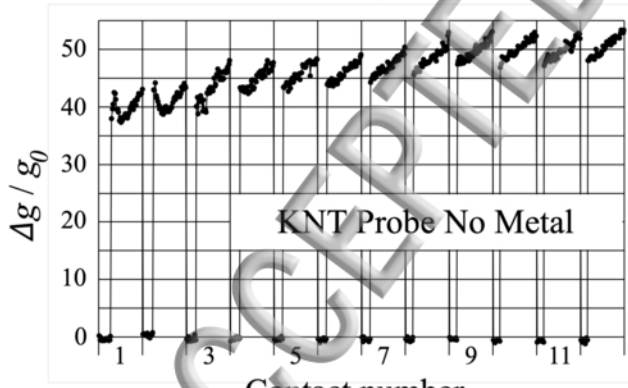
KNT Probe No Metal
Δg / g0
Contact number

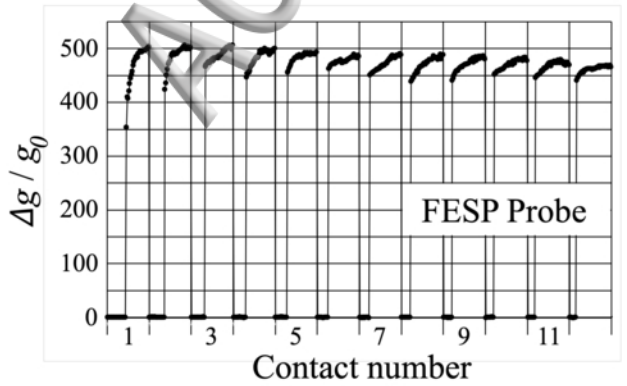
FESP Probe
Δg / g0
Contact number

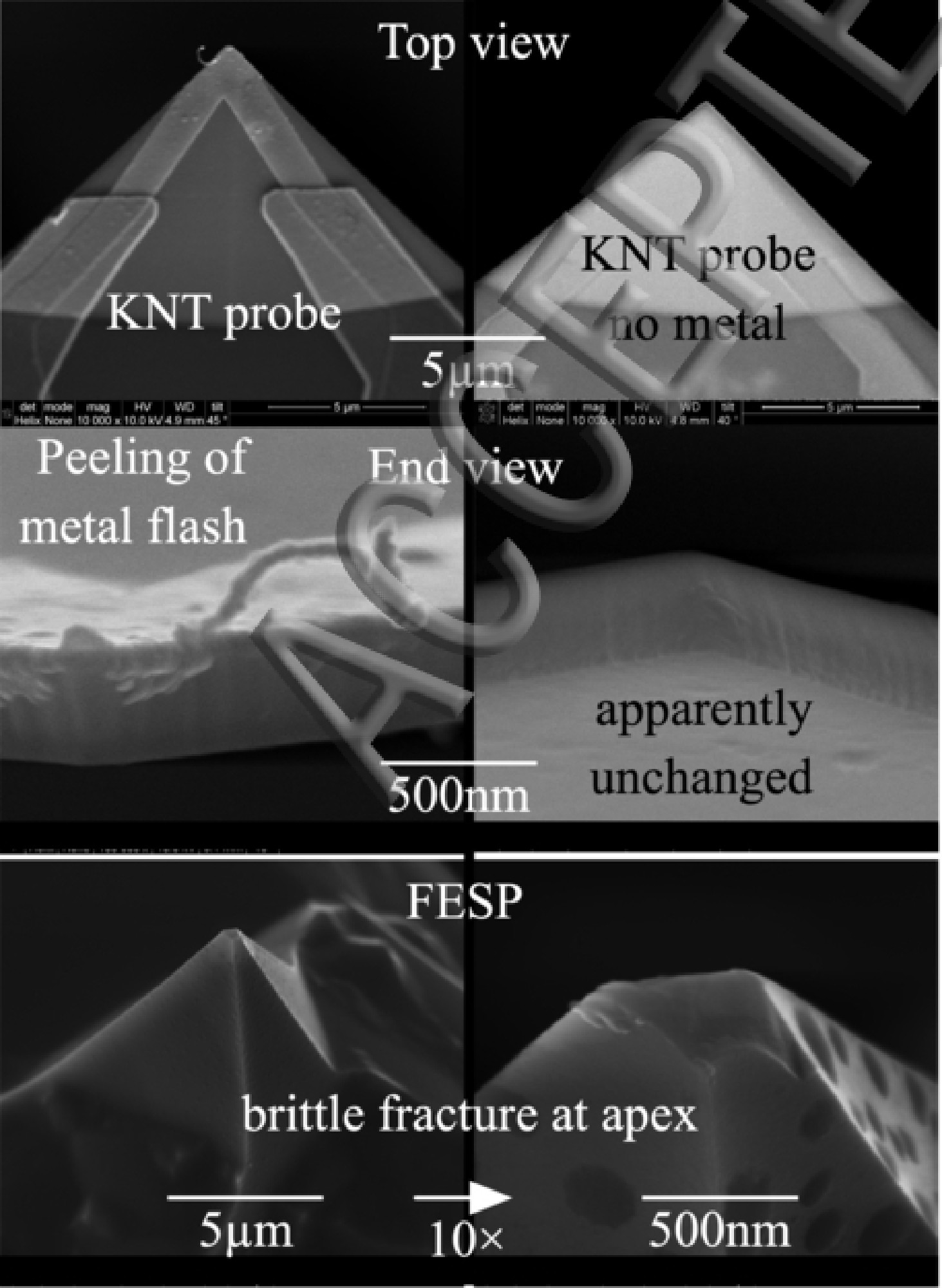
Top view
KNT probe
KNT probe
no metal
5µm
Peeling of
metal flash
End view
apparently
unchanged
500nm
FESP
brittle fracture at apex
5µm
10×
500nm